JKAU: Sci., **Vol. 18,** pp: 63-79 (2006 A.D. / 1427 A.H.)

Atomic Emission Rate Inside a Quantum Resonator

S. Al-Awfi
Department of Physics, Taibah University,
Al-Madina Al-Munawwarah, Saudi Arabia

Abstract. We present a general formalism for studying the emission rate of an atom inside a high Q-factor quantum cylindrical resonator. The electromagnetic field structure inside such closed resonator is derived. Then the cavity modes are quantised, allowing the position-dependent atomic emission rate to be calculated. Depending on the circumstances, the atomic emission rate may be increased or reduced, and in extreme cases is completely suppressed. Especially, in the quantum size system, the atomic emission rate is possible only via a few cavity modes. The calculations are carried out for the sodium atoms immersed in an empty quantum size resonator.

1. Introduction

The last decade or so has witnessed a rapid increase in the study, design and fabrication of electromagnetic cavities, which can modify the nature and strength of the interaction of light with matter. Since the pioneering work of Purcell[1] much research has been carried out on the cavity quantum electrodynamics 'CQED' effects, especially, on the modification of atomic emission rate and its practical consequences for atoms immersed in various dielectric media and cavity structure of different shapes and sizes[2-7]. However, CQED is still one of the most rapidly developing areas of physics and promise to lead to some of the most important future applications[8-9].

We concentrate here on the atomic emission rate inside an empty resonant cavity. This type of structure, in general, consists of a region of finite extension enclosed by walls and filled with a dielectric. This cavity will resonate at frequencies corresponding to certain configurations of the fields. We have considered this type of structure for the following reasons. Firstly, despite the fact that the electromagnetic modes of a cylindrical resonators are well known, as

far as we know for this system neither the quantisation of the modes nor the spatially-varying atomic emission rate have been calculated before. Although such system has been used as a good environment to obtain an electrostatic quadrupole potential with sufficient quality to observe a single trapped electron[10].

Secondly, the cylindrical resonator is a natural extension to the circular waveguide system, when the axial direction (along the cylinder) of the cylindrical resonator becomes large. The circular waveguide was recently the subject of many studies in the context of CQED[11-13]. The cylindrical resonator also gives a natural extension to the parallel plates system, when the radius of the circular base of cylindrical cavity becomes large, which has also been the subject of extensive studies[2-5]. As will be seen, these limits provide a useful check of the calculation. We expect that in the small volume, especially when a and l become comparable or less than the electric dipole transition wavelength λ_0, the atomic emission rate becomes more restricted than the waveguide case[13]. Finally, we are also interested in this type of system because, it is currently receiving attention in the context of quantum optics and non-linear optics domains, in particular, a one-atom laser[14] and an optical trapping of individual atoms by the mechanical forces associated with single photon[15-17].

The main objective of this paper is to evaluate the atomic emission rate for this situation and explore the factors that influence the suppression and enhancement of this rate. The plan of the paper is as follows. In section 2 we present the physical model of this study and then briefly derive the electromagnetic fields inside such model. In section 3 we briefly show the Hamiltonian formalism and we summarise the procedure leading to the quantised electromagnetic modes inside a cylindrical resonator. Section 4 deals with formalism for the evaluation of the atomic emission rate of a dipole placed inside the cylindrical resonator. The results of the theory are given in section 5 and are illustrated with reference to typical situations involving sodium atoms in a quantum size resonator. Section 6 contains comments and conclusions.

2. Field Structure in a Closed Resonator

2.1 Physical Model

The basic physical model focussed on here is in the form of an empty cylindrical resonator, as illustrated in Fig. 1. As shown in this figure, the resonator is assumed to have volume $\pi a^2 l$ where a and l are the radius of the circular base and the length of the cylinder respectively. The walls of such closed resonator are assumed to be a perfect conductor and so exclude all electromagnetic fields from their interior. The standard electromagnetic boundary conditions apply such that the tangential components of the electric field vector and the mag-

netic field vector must vanish at every point on the circular base and on the cylinder surface. As a result of these properties, the energy injected during a very short time can remain stored in a system for a very long time in comparison with the period, which means a very high quality factor Q. This type of resonator can be formed by placing conducting plates at both ends of a cylindrical waveguides with circular cross section.

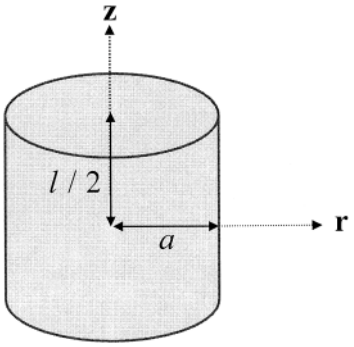

Fig. 1. Schematic drawing of the hollow cylindrical resonator. The resonator walls are assumed to be perfectly conducting.

2.2 Normal Modes

The modes of an empty cylindrical resonator are well known from microwave theory, and the derivation was outlined in detail in Ref. [18]. We consider the wave equations for the fields **E** and **B**, and assuming a time harmonic variation $\exp(i\omega t)$, we reduce these to Helmholtz equations for the two fields:

$$\nabla 2\,\mathbf{E} + \mu_0\varepsilon_0\omega\mathbf{E} = 0, \qquad \nabla^2\mathbf{B} + \mu_0\varepsilon_0\omega\mathbf{B} = 0 \tag{1}$$

Because we are dealing with cylindrical geometry, it is more convenient to express ∇^2 in cylindrical coordinates r, ϕ and z in order to impose the boundary conditions,

$$\nabla^2 = \frac{1}{r}\frac{\partial}{\partial r}\left(r\frac{\partial}{\partial r}\right) + \frac{1}{r^2}\frac{\partial^2}{\partial\phi^2} + \frac{\partial^2}{\partial z^2} \tag{2}$$

$$\mathbf{E} = E_r\hat{r} + E_\phi\hat{\phi} + E_z\hat{z} \quad , \quad \mathbf{B} = B_r\hat{r} + B_\phi\hat{\phi} + B_z\hat{z} \tag{3}$$

It is well known that in cylindrical coordinates the operation of ∇^2 on **E** and **B** will couple r and ϕ components together but leave z component uncoupled. However, this can be solved by considering Mexwell's equations for **E** and **B**. It can be shown that the solution to the scalar equation[18]

$$(\nabla^2 + \mu_0\varepsilon_0\omega)\ \Psi\ (r, \phi, z) = 0 \tag{4}$$

is given by:

$$\Psi\ (r, \phi, z) = \Psi_0 J_n\ (hr) \cos\ (kz) \exp \pm in\phi \tag{5}$$

where Ψ denotes either **E** or **B**, Ψ_0 is, as yet, undetermined constant and $J_n\ (hr)$ is the Bessel function of the first kind. Finally the separation constants h and k are connected by the relation

$$h^2 + k^2 = \mu_0\varepsilon_0\omega \tag{6}$$

The transverse field components E_r, E_ϕ, B_r and B_ϕ, in general, can be expressed as functions of E_z and B_z only. We may thus consider any solution that is a linear combination of solutions for the two distinct cases $E_z = 0$ and $B_z = 0$, the so-called ordinary (*TE*) and extraordinary (*TM*) modes respectively.

2.2.1 Ordinary Modes (TE)

To determine the *TE* modes, one solves the transverse field components for the B_z component:

$$E_z\ (r, \phi, z) = 0 \tag{7}$$

$$B_z\ (r, \phi, z) = \Psi_0^{TE} J_n\ (hr) \cos\ (kz) \exp \pm in\phi \tag{8}$$

and derives the other components by using

$$E_\phi = -\frac{i\omega}{h^2}\ \frac{\partial B_z}{\partial r}\ , \qquad E_r = -\frac{\omega n}{h^2}\frac{B_z}{r} \tag{9}$$

$$B_r = -\frac{ik}{h^2}\ \frac{\partial B_z}{\partial r}\ , \qquad B_\phi = -\frac{kn}{h^2}\frac{B_z}{r} \tag{10}$$

To determine h, we apply the boundary conditions at $r = 0$, $r = a$, $z = 0$ and $z = l$, which lead to two conditions. Firstly we find that $\sin kl = 0$, which requires that $k_\ell\, l = \ell\pi$ where $\ell = 0,1,2,3,...$ Secondly $J_n'\ (h_{nm}r) = 0$, so that $J_{nm}'\ a = \beta_{nm}$ is the root of $J_n'\ (\beta_{nm}) = 0$. Thus, the total mode functions for the ordinary modes (*TE*) can be written as:

$$\mathbf{E}_{TE}(n, m, \ell, \mathbf{R}, t) = \Psi_{nm\ell}^{TE}\begin{bmatrix} i\ \cos(k_\ell z)J_n'(h_{nm}'r)\ \ \hat{\phi} \\ -\dfrac{n}{h_{nm}'r}\sin(k_\ell z)J_n(h_{nm}'r)\ \ \hat{\mathbf{r}} \end{bmatrix}\ e^{\pm in\phi}e^{i\omega_{nm\ell}^{TE}t} \tag{11}$$

Therefore the dispersion relation $\omega_{nm\ell}^{TE}$ of the ordinary mode is

$$\omega_{nm\ell}^{TE} = c\left(\left(\frac{\ell\pi}{l}\right)^2 + \left(\frac{\beta_{nm}}{a}\right)^2\right)^{1/2} \tag{12}$$

Eq (12) shows that the resonant frequency increases as the order of mode becomes higher. The TE_{111} mode is the fundamental mode if the condition $l / a >$ 2 is satisfied. However, the TE_{011} mode were only E_ϕ is non-zero E_r vanishes is the great practical interest mode.

2.2.2 Extraordinary Modes (TM)

For the *TM* modes and with B_z $(r, \phi, z) = 0$, E_z is given by

$$E_z\,(r, \phi, z) = \Psi_0^{TM} J_n\,(hr) \cos\,(kz) \exp \pm in\phi \tag{13}$$

The remaining field component can be obtained using:

$$E_\phi = -\frac{nk}{h^2}\frac{E_z}{r}\,, \qquad E_r = -\frac{ik}{h^2}\frac{\partial E_z}{\partial r} \tag{14}$$

$$B_\phi = \frac{i\mu_0\varepsilon_0\omega}{h^2}\frac{\partial E_z}{\partial r}\,, \quad B_r = \frac{n\mu_0\varepsilon_0\omega}{h^2}\frac{E_z}{\partial r} \tag{15}$$

To determine h, we require $J_n\,(h_{nm}r) = 0$, so that $h_{nm}a = \alpha_{nm}$ where α_{nm} are the roots of $J_n\,(\alpha_{nm}) = 0$. Thus, the total mode functions for the extraordinary modes (*TM*) can be written as:

$$\mathbf{E}_{TM}(n,m,\ell,\mathbf{R},t) = \Psi_{nm\ell}^{TM}\begin{bmatrix} -\dfrac{k_\ell n\ \cos(k_\ell z)}{h_{nm}^2 r}\ J_n(h_{nm}r)\hat{\boldsymbol{\phi}} \\ +\dfrac{k_\ell\ \cos(k_\ell z)}{h_{nm}}\ J_n'(h_{nm}r)\hat{\mathbf{r}} \\ +iJ_n(h_{nm}r)\ \sin(k_\ell z)\hat{\mathbf{z}} \end{bmatrix} e^{\pm in\phi}e^{-i\omega_{nm\ell}^{TM}t} \tag{16}$$

where $h_{nm}a = \alpha_{nm}$ and α_{nm} are the roots of $J_n(\alpha_{nm}) = 0$. Therefore the dispersion relation $\omega_{nm\ell}^{TM}$ of the extraordinary mode is

$$\omega_{NM\ell}^{TM} = c\left(\left(\frac{\ell\pi}{l}\right)^2 + \left(\frac{\alpha_{nm}}{a}\right)^2\right)^{1/2} \tag{17}$$

It is clear that the resonant frequency increases as the order of mode becomes higher. The TM_{010} mode is the fundamental mode if the condition $l / a < 2$ is satisfied, all electric field components being zero except *Ez*.

3. QED in a Cavity Resonator

3.1 Hamiltonian Formalism

The quantum system consists of an atom of mass M, characterised by its electric dipole moment **d**, of oscillation frequency ω_0, interacting with the electromagnetic field. An appropriate Hamiltonian is given by:

$$H = H_A + H_{field} + H_{\text{int}} \tag{18}$$

where H_A and H_{field} are the unperturbed Hamiltonian for the atom and field

$$H_A + \frac{\mathbf{P}^2}{2M} + U(\mathbf{R}) \tag{19}$$

$$H_{field} = \hbar\omega\, a^+ a \tag{20}$$

Here **P** and **R** are the momentum and position vectors of the atomic centre of mass which is assumed to be subject to a general potential $U(\mathbf{R})$. In the two-level approximation, the internal motion of the atom involves only two states: $|e\rangle$, of energy E_e, and $|g\rangle$, of energy E_g, such that $E_e - E_g = \hbar\omega_0$. The operators a^+ and its conjugate are the creation and annihilation operators for the specified field mode, respectively.

The interaction Hamiltonian H_{int} in Eq. (18), describes the coupling of the atom to the electromagnetic field and is given in the electric dipole approximation by:

$$H_{\text{int}} = -\,\mathbf{d}.\,\mathbf{E}\,(\mathbf{R}) \tag{21}$$

were $\mathbf{E}(\mathbf{R})$ is the electric field evaluated at the position **R** of the atom. The atomic dipole moment operator may be written as:

$$\mathbf{d} = \langle \mathbf{d} \rangle_{eg}\,(\pi + \pi^+) \tag{22}$$

The operators π and π^+ are the lowering and raising operators for the internal atomic states and $\langle \mathbf{d} \rangle_{eg}$ is the dipole matrix element of the atomic transition.

3.2 Quantised Fields

We next quantise the field to describe the interaction with an atomic system. The total quantised electric and magnetic field operators can be written as follows[19]:

$$\mathbf{E}(\mathbf{R},t) = \sum_{\eta=(TE,TM)} \sum_{nm\ell} \left\{ a_\eta(m,n,\ell)\tilde{\mathbf{E}}_\eta(m,n,\ell,\mathbf{R},t) + h.c. \right\} \tag{23}$$

$$\mathbf{B}(\mathbf{R},t) = \sum_{\eta=(TE,TM)} \sum_{nm\ell} \left\{ \left(\frac{1}{i\omega(m,n,\ell} \right) a_\eta(m,n,\ell)\vec{\nabla} \times \tilde{\mathbf{E}}_\eta(m,n,\ell,\mathbf{R},t) + h.c. \right\} \tag{24}$$

where *h.c.* stands for 'Hermitean conjugate' and we have expressed the position vector in components form by writing $\mathbf{R} = (r, \phi, z)$. The operator $a_\eta(m, n, \ell)$ is the boson operator for the field mode of polarisation $\eta(= TE, TM)$ characterised by integer quantum numbers m, n and ℓ. The relevant commutation relations are

$$\left[a_\eta(m, n, \ell), a^+_{\eta'}(m', n', \ell')\right] = \delta_{\eta\eta'}\ \delta_{mm'}\ \delta_{mn'}\ \delta_{\ell\ell'} \tag{25}$$

Hence, the two normalisation factors $\Psi^{TE}_{nm\ell}$ in Eq. (11) and $\Psi^{TE}_{nm\ell}$ in Eq. (16) are obtained respectively as:

$$\psi^{TE}_{nm\ell} = \left(\frac{2\hbar\omega\beta^2_{nm}}{\xi_{nm\ell}\varepsilon_o V(\beta^2_{nm} - n^2)\ J^2_n(\beta_{nm})}\right)^{\frac{1}{2}} \tag{26}$$

$$\psi^{TE}_{nm\ell} = \left(\frac{2c^2\hbar\alpha^2_{nm}}{\xi_{nm\ell}\varepsilon_o V(\beta^2_{nm} - n^2)\ J^2_n(\beta_{nm})}\right)^{\frac{1}{2}} \tag{27}$$

where V is the quantum volume of the resonator, with $\zeta_{nm\ell}$ that arises from the sinusoidal azimuthal nature of the mode functions and it is such that $\zeta_{010} = ¼$, $\zeta_{011} = ½ = \zeta_{110}$, and $\zeta_{nm\ell} = 1$ for n, m and ℓ satisfying $n \geq 1$, $m \geq 1$ and $\ell \geq 1$.

The total Hamiltonian for the electromagnetic fields within the cylindrical resonator is

$$H_{field} = \frac{1}{2}\int_0^l dz \int_0^a r dr \int_0^{2\pi} d\phi \left\{\varepsilon_0 E^2(\mathbf{R}, T) + \frac{1}{\mu_0} B^2(\mathbf{R}, t)\right\} \tag{28}$$

The factors $\Psi^{TE}_{nm\ell}$ and $\Psi^{TE}_{nm\ell}$ defined in Eq. (26) and (27) are fixed by the usual quantisation requirement that H_{field} reduces to the canonical form

$$H_{field} = \frac{1}{2}\sum_{\eta(=TE,TM)}\sum_{nm\ell}\hbar\omega^\eta_{nm\ell}\left\{a_\eta(n,m,\ell)a^+_\eta(n,m,\ell) + a^+_\eta(n,m,\ell)a_\eta(n,m,\ell)\right\} \tag{29}$$

From the above discussion, we note that the structure of electromagnetic fields in the closed resonator is truly the primary difference compared to the case of an atom radiating in free space: Firstly, it exhibits a discrete frequency spectrum, so we can easily excite a specific mode in a cavity. Secondly, the field strength depends on position which gives rise to the position-dependent atomic emission rate. At the moment, with the electromagnetic modes quantised, one can evaluate the atomic emission rate and explore its variation with the controllable parameters of the system.

4. Atomic Emission Rate

Having determined the normalisation factors of the fields $\Psi^{TE}_{nm\ell}$ and $\Psi^{TE}_{nm\ell}$, our new task is the evaluation of the atomic emission rate by dipole emitter,

considering a two-level system with the ground stage $|g\rangle$ and the excited state $|e\rangle$ separated by transition frequency $\omega_0 = (E_e - E_g) / \hbar$. For an electric dipole of moment vector **d** located at an arbitrary point **R** = (r, ϕ, z) within the resonator, the atomic emission rate is given by Fermi's golden rule as:

$$\Gamma(\mathbf{R}) = \frac{2\pi}{\hbar} \sum_{\eta=(p,s)} \sum_{nm\ell} \left| \left\langle e;\{0\} \right| -\mathbf{d}.\tilde{\mathbf{E}}(\mathbf{R}) \left| g;\{nm\ell,\eta\} \right\rangle \right|^2 \delta\left(E_e - E_g - \hbar\omega^{\eta}_{nm\ell}\right) \qquad (30)$$

which gives the rate of transition from the $|e\rangle$ to $|g\rangle$ by the emission of all possible single quanta of cavity modes with state $|\{nm\ell,\ \eta\}\rangle$ of frequency $\omega^{\eta}{}_{nm\ell}$ and polarisation η. The vacuum state is represented by $|\{0\}\rangle$. The delta function $\delta\left(E_e - E_g - \hbar\omega^{\eta}_{nm\ell}\right)$ signifies the presence of the cavity resonances at frequencies given by Eq. (12) and (18). The best representation of the delta function in the closed resonator case is possible by assuming that there is a small amount of cavity loss, then it can be introduced as a limit of a Lorentzian function

$$\delta\left(\omega_0 - \omega^{\eta}_{nm\ell}\right) \to \left\{ \frac{1}{2\pi} \frac{1\ /\ \tau}{\left(\omega_0 - \omega^{\eta}_{nm\ell}\right)^2 + (1\ /\ \tau)^2} \right\} \equiv \wedge_{nm\ell} \qquad (31)$$

where τ is the cavity lifetime. Then, in the case of perfectly conducting wall (*i.e.*, *reflectivity* =), we have $\tau \to \infty$ and the delta functions are recovered. While as the reflectivity of the cavity walls moves away from unity, the frequency resonance of the cavity decreases, and the delta functions broaden out. The overall losses of a cavity mode with eigen-frequency $\omega^{\eta}_{nm\ell}$ are frequently obtained by Q-factor[20]

$$Q = \tau\omega^{\eta}_{nm\ell} \qquad (32)$$

In a cavity of high Q-factor, an atom can interact resonantly with an isolated mode of the electromagnetic field, a case somewhat different from the free space, where the atom is coupled to a continuum of field nodes, which act as a dissipative reservoir. Depending on the time of cavity damping as compared to free space, one can distinguish between two cases; the good cavity limit which is characterised by slower damping and a bad cavity limit with a faster damping[21].

It is worth noting that the resonator frequency spectrum determined by Eq. (12) and (17) comprises two sets of discrete branches, one for each type of polarisation η = (*TE*, *TM*). A frequency branch is labelled by three fixed integers m, n and ℓ. Since $\omega^{\eta}_{nm\ell}$ depends on the cavity dimensions a and l entering via h_{nm}, h'_{nm} and k_ℓ, Eq. (12) and (17) conceal the dependence on the chosen values of a and l. From the special case illustrated in Table 1 ($l = 2a \approx 1\mu$m), we can

see that the frequency separation $\Delta\omega_\eta$ between the adjacent modes is quite large. Thus if the dipole frequency is less than ω_{TM}^{101}, emission is only possible by the two modes; ω_{TM}^{011}, and ω_{TM}^{110}. In the case $l > 2a$, the lowest resonance frequency is the ω_{TM}^{111} while ω_{TM}^{010} is the lowest resonance frequency when $l < 2a$. These notations are very important in the quantum size domain because they determine the number and the order of the allowing modes.

Table 1. Frequencies of some modes when $l = 2a \approx 1\ \mu$m.

***TE*-modes**	ω_{TE}^{nml}	***TM*-modes**	ω_{TE}^{nml}
TE_{011}	$1{\cdot}103 \times 10^{14}$	TM_{010}	$3{\cdot}607 \times 10^{14}$
TE_{110}	$2{\cdot}762 \times 10^{14}$	TM_{110}	$5{\cdot}747 \times 10^{14}$
TE_{210}	$4{\cdot}581 \times 10^{14}$	TM_{120}	$7{\cdot}703 \times 10^{14}$
TE_{010}	$5{\cdot}747 \times 10^{14}$	TM_{011}	$10{\cdot}087 \times 10^{14}$
TE_{111}	$9{\cdot}816 \times 10^{14}$	TM_{111}	$11{\cdot}034 \times 10^{14}$
TE_{211}	$10{\cdot}047 \times 10^{14}$	TM_{121}	$12{\cdot}168 \times 10^{14}$

In general, the procedure for the evaluation of the atomic emission rate based on Eq. (30) can be outlined as follows. Contributions from *TE* and *TM* modes are carried out separately. After evaluating the squared matrix element, the use of Eq. (31) facilitates the evaluation of the delta function. We are then left with two sums over integers, n, m and ℓ which can be calculated numerically. We may cast the final results of the atomic emission rates for a given dipole orientation, in term of the variable

$$\sigma = \frac{a}{\lambda_0} \tag{33}$$

where λ_0 is the free space transition wavelength and we may also simplify the results by considering the ratio of atomic emission with that in free space Γ_0, which allow us to eliminate the atomic matrix elements

$$\Gamma_0 = \frac{d^2\omega_o^3}{3\pi\ \hbar\varepsilon_0 c^3} \tag{34}$$

The final results for each of the three different Γ_z, Γ_r and Γ_ϕ will be given here as follow:

(a) For the z dipole

$$\Gamma_z(\mathbf{R}) = \Gamma_0 \sum_{nm}^{[2\pi\sigma][2l\ /\ \lambda]} \sum_{\ell} \Theta\ \cos^2(k_\ell z) \frac{\alpha_{nm}^2}{\sigma^2 J_{n+1}^2(\alpha_{nm})} J_n^2(h_{nm} r) \tag{35}$$

(b) For the r dipole

$$\Gamma_r(\mathbf{R}) = \Gamma_0 \sum_{nm}^{[2\pi\sigma]} \sum_{\ell}^{[2l/\lambda]} \Theta \ \sin^2(k_\ell z) \left\{ \begin{array}{l} \dfrac{a^2 k_\ell^2}{\sigma^2 J_{n+1}^2(\alpha_{nm})} J_n'^2(h_{nm} r) \\ + \dfrac{2n^2 a^2}{(\beta_{nm}^2 - n^2) J_n^2(\beta_{nm})} J_n^2(h_{nm}' r) \ / \ r^2 \end{array} \right\} \tag{36}$$

(c) For the ϕ dipole

$$\Gamma_\phi(\mathbf{R}) = \Gamma_0 \sum_{nm}^{[2\pi\sigma]} \sum_{\ell}^{[2l/\lambda]} \Theta \ \sin^2(k_\ell z) \left\{ \begin{array}{l} \dfrac{a^4 k_\ell^2 n^2}{\sigma^2 \alpha_{nm}^2 J_{n+1}^2(\alpha_{nm})} J_n^2(h_{nm} r) \ / \ r^2 \\ + \dfrac{2\beta_{nm}^2}{(\beta_{nm}^2 - n^2) J_n^2(\beta_{nm})} J_n'^2(h_{nm}' r) \end{array} \right\} \tag{37}$$

where the dimensionless factor Θ is given by

$$\Theta = \frac{3\lambda_0^3 c \Lambda_{nm\ell}}{4\varsigma_{nm\ell} V} \tag{38}$$

These results can now be explored for typical situations involving sodium atoms in cylindrical resonator. Our main concern here is the quantum effects of such system and to see such effects one should try to make the system size comparable or smaller than the thermal de Broglie wavelength of the atoms. However, a micrometers-sized system might be the smallest one could envision making.

Before we consider the quantum regime, we mention that it is very easy to check the results by using a particularly simple asymptotic limit arising when a and l increase to infinity. In this situation the results in Eq. (35), (36) and (37) will yield the atomic emission rate in free space. On the other hand, the results will yield the atomic emission rate in the parallel plate system when a or l increase to infinity and keeping another one fixed with some change due to the curvature of the cylinder. The results will yield the atomic emission rate in the circular waveguide limit when l increases to infinity and a fixed. These properties are well known in CQED literature and so we will not go any further here except the foremost limit, which is important to determine the no decaying region.

5. A Neutral Atom in a Quantum Resonator System

To have a good impression about the orders of values, it is instructive to concentrate on a typical physical case. We consider the situation of a sodium atom and focus on its $3^2 s_{1/2} \leftrightarrow 3^2 p_{3/2}$ transition ($\lambda_0 = 589nm$). The value of the dipole matrix element associated with this transition is $d \approx 2.6ea_B$, which is compatible with the measured free space lifetime of $\tau \approx 16.3\ ns$ (or $\Gamma_0 = 6.13 \times 10^7\ s^{-1}$).

For our aim, we will suppose that $l = 2a \equiv L$. By simple algebraic, we can show that the results from Eq. (36) and (37) are the same at the centre of an empty resonator (or at $r = 0$). In Fig. 2, we plot the variation of the atomic emission rate as a function of the normalised distance L / λ_0 for an atom at the centre of the resonator, *i.e.*, at the point ($l / 2$, a), with the atomic dipole, in turn, along the three directions. It is clear that, there is a 'cut-off' value of L below which there is no atomic emission. In each case the rates oscillates with increasing L before approaches the free space value at L.

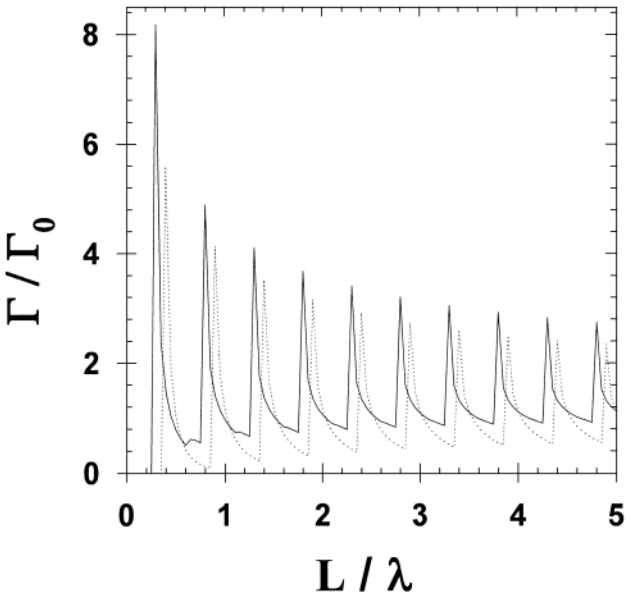

Fig. 2. Variation of the atomic emission rate for an atom placed at the centre of closed resonator as a function of the ratio L / λ. The lines show the emission when a dipole is oriented along z while the dots show it when a dipole is oriented along r(*or* ϕ) – *directions.*

The contribution of every mode to the atomic emission rate also depends on the atom location respect to the internal surfaces of the resonator. To illustrate that we should consider the spatial distribution of the field in that mode in two situations. Firstly, when the atom takes different locations on the normal axis of cylinder r / λ_0 with fixed distance from the circular base at $l / 2$, as shown in Fig. 3. Of course, in this case, we can consider Γ_z and the parallel polarised while Γ_r and Γ_ϕ represent the normal polarised. Secondly, when the atom locates at altered places on the longitudinal cylinder axis z / λ_0 with fixed distance from lateral surfaces at a, as shown in Fig. 4. It is clear that Γ_z represents the normal polarised while Γ_r and Γ_ϕ represent the parallel polarised.

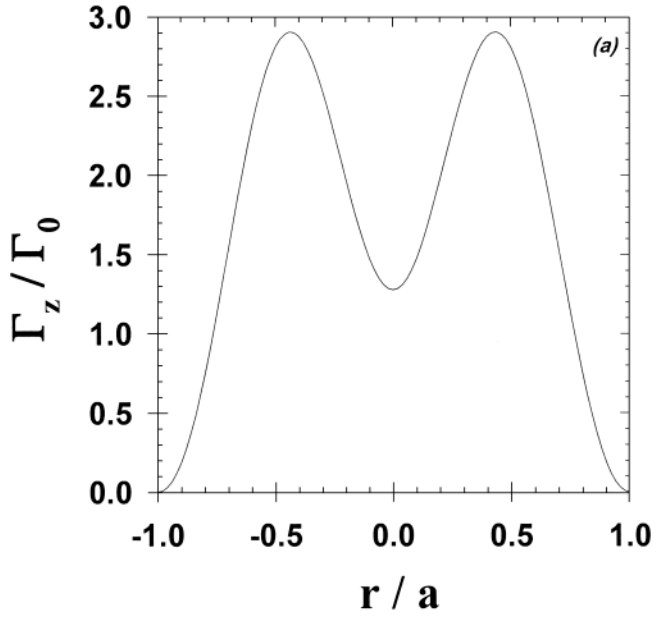

Fig. 3a. The cross-section distribution plots for the atomic emission rate when the atom moves on the diameter of the resonator. Atomic dipole is oriented along: (a) *z*, (b) *r*, (c) ϕ.

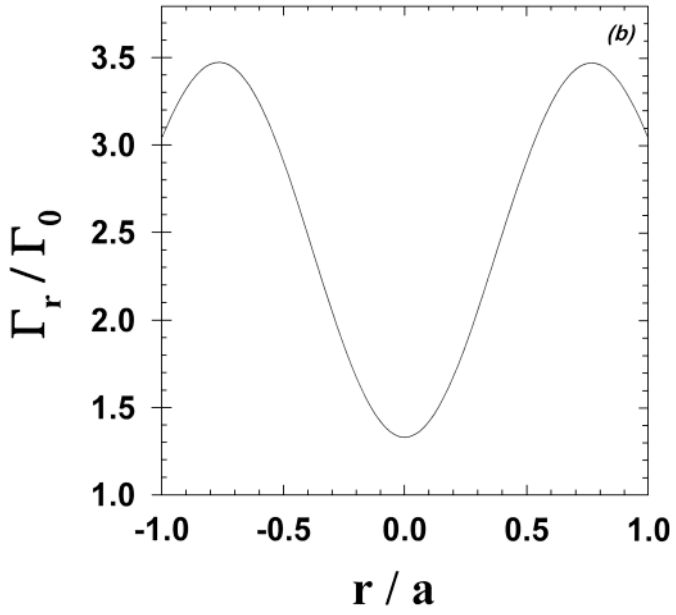

Fig. 3b

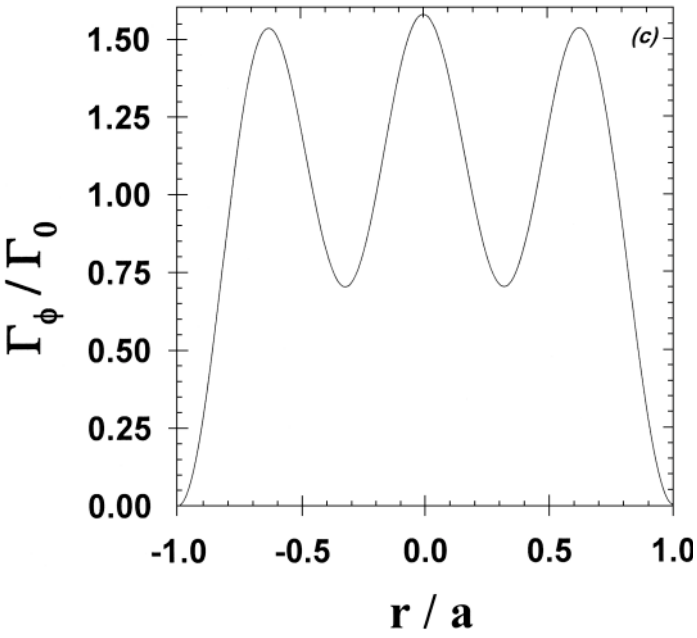

Fig. 3c

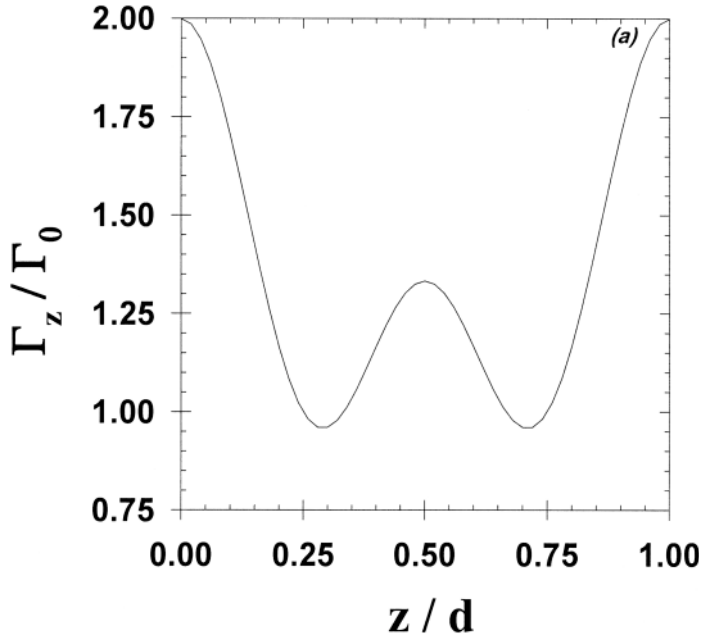

Fig. 4a. The cross-section distribution plots for the atomic emission rate when the atom moves on the length of the resonator. Atomic dipole is oriented along: (a) *z*, (b) *r*, (c) ϕ.

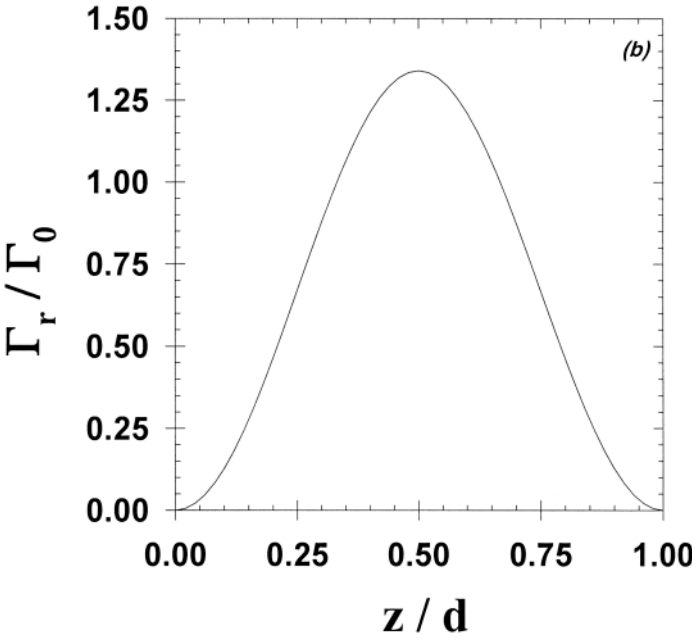
(b)
1.50
1.25
1.00
0.75
0.50
0.25
0.00
Γr / Γ0
0.00
0.25
0.50
0.75
1.00
z / d

Fig. 4b

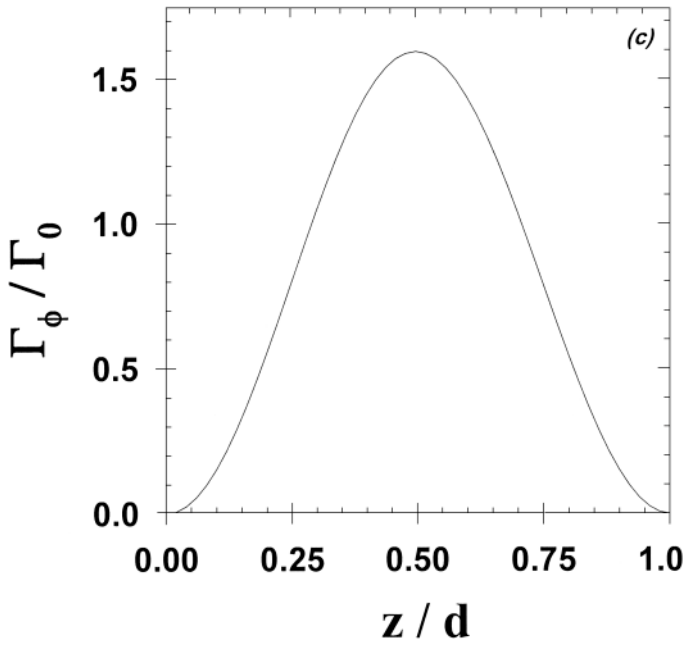
(c)
1.5
1.0
0.5
0.0
Γϕ / Γ0
0.00
0.25
0.50
0.75
1.0
z / d

Fig. 4c

As shown, at the surface of the resonator, the atomic emission rates take different value for each case, as consequence to the curvature of the cylindrical surface. In Fig. 4, Γ_z is enhanced by a factor $2\Gamma_0$, which means that it represented exactly the well-known results of the dipole normal to the flat conducting surface. While the variations of Γ_r and Γ_ϕ are nearly the same with each other and they represent the result of the dipole parallel to the flat surface. On the other hand, in Fig. 3, Γ_r represented the case of the dipole normal to surface and enhanced by a factor more than $3\Gamma_0$, as consequence to the curvature of the cylindrical surface. While the variations of Γ_z and Γ_ϕ are nearly the same with each other and they represent the case of the dipole parallel to the surface.

It can be deduced from these figures that the enhancement of the atomic emission rate is larger when the atom is near a curvature surface rather than a near a flat surface. Finally, it is important to note that, because of the quantum system size ($a = L / 2 = 0{\cdot}9\ \lambda_0$) chosen for illustration purposes in Fig. 3 and 4; the atomic emission rates arise from at most three modes of the cavity.

6. Comments and Conclusions

In conclusion we have examined in detail the atomic emission rate of atoms immersed in a quantum size resonator with circular cross-section. The resonator modes are first quantised by following the standard procedure, incorporating the boundary conditions at the system walls, which permitted the position-dependent atomic emission rate to be evaluated for an electric dipole within the resonator. Advantageous limits of the atomic emission rate have been derived. We have been able to recover the results appropriate for the free space case when l and a become large.

We have also presented that in the limit of small size, especially when the length of the cavity l and its radius a become less than λ_0, the atomic emission process is possible only via a few cavity modes. Such systems forming the quantum dot cavities promise to lead to important future applications in Bose-Einstein condensation and quantum information processing[15-17].

We have focused here only on system characterised by two distinct features. First the walls of the resonator are assumed to have infinite conductivity leading to a situation of a perfect efficiency with no power loss. In actuality, there are some losses, which decrease the quality factor Q of the resonator. Secondly, the resonator is of a cylindrical geometry with smaller surface area by 8·2% as compared to a rectangular resonator at the same volume. This will lead to a lower power loss and a higher quality factor Q[20].

Furthermore to its intrinsic value, the atomic emission rate in such system is very significant for the theory of an optical trapping of individual atoms by the

mechanical forces associated with single photons. This kind of trapping represents elementary quantum systems that are well isolated from the environment. Recently, many experimental studies have considered the open geometries for atom resonator such as two-plate systems or waveguides. Such kinds of systems have clear advantages when it comes to loading the trap and manipulating the atoms (*e.g.*, cooling, mode selecting). They suffer, however, from the problem that is relatively easy for the atoms to escape. While the close resonator confines atom in all directions. Therefore, we can excite a particular mode in a close resonator from a tiny hole (or iris) at an appropriate location in the resonator walls. This hole may be connected directly to the source or by a waveguide, which is commonly used for coupling mode to a close resonator. Moreover, as a consequence of the standing waves pattern within a resonator, the atom is only subjected to a transverse dipole potential while the dissipative force is equal to zero (because of standing waves $\theta = 0$ and for running wave $\theta = \mathbf{k.r}$).

References

[1] **Purcell, E.M.,** *Phys. Rev.*, **69:** 681 (1946).
[2] **Barton, G.,** *Proc. Roy. Soc. Lond.*, **A367:** 117 (1979).
[3] **Hinds, E.,** Adv. Atom. Mol., *Opt. Phys.*, **2:** 1 (1993).
[4] **Dutra, S.M.** and **Knight, P.L.,** *Opt. Comm.*, **117:** 256 (1995).
[5] **Dutra, S.M.** and **Knight, P.L.,** *Phys. Rev.*, **A53:** 3587 (1996).
[6] **Nha, H.** and **Jhe, W.,** *Phys. Rev.*, **A56:** 2213 (1997).
[7] **Al-Awfi, S.** and **Babiker, M.,** *Phys. Rev.*, **A58:** 4768 (1998).
[8] **Wright, E.M., Jessen, P.S.** and **Lapeyere, G.J.,** *Opt. Comm.*, **129:** 423 (1996).
[9] **Ol'Shanii, M., Ovchinnkov, Y.** and **Letokhov, V.,** *Opt. Comm.*, **98:** 77 (1993).
[10] **Gabrielse, G.** and **Tan, J.,** *Adv. Atom. Mol., Opt. Phys.*, **2:** 267 (1994).
[11] **Rippin, M.A.** and **Knight, P.L.,** *J. Mod. Opt.*, **47:** 807 (1996).
[12] **Kakazu, K.** and **Kim, Y.S.,** *Prog. Theor. Phys.,* **96:** 883 (1996).
[13] **Babiker, M.** and **Al-Awfi, S.,** *Rev.*, **A61:** 033401-1, 13 (2000).
[14] **Dowling, J.P.** and **Gea-Banacloche, J.,** *Adv. Atom. Mol. and Opt. Phys.*, **37:** 1 (1996).
[15] **Mundt, A., Kreuter, A., Becher, C., Leibried, D., Eschner, J., Schmidt-Kaler, F.** and **Blatt, R.,** *Phys. Rev. Lett.*, **89:** 103001 (2002).
[16] **Ye, J., Vernooy, D.** and **Kimble, H.,** *Phys. Rev. Lett.*, **83:** 4987 (1999).
[17] **Doherty, A., Lynn, T., Hood, C.** and **Kimble, H.,** *Phys. Rev.*, **A63:** 013401 (2000).
[18] **Cheng, D.K.,** *'Field and Wave Electromagnetics'* (Addison-Wesley, 1989).
[19] **Allen, L., Babiker, M., Lai, W.** and **Lembessis, V.,** *Phys. Rev.,* **A54:** 4259 (1996).
[20] **Jackson, J.,** *'Classical Electrodynamics'*, Addison-Wesley (1975).
[21] **Meschede, D.,** *Phys. Rep.*, **211:** 5,202 (1992).
[22] **Adams, C.** and **Riss, E.,** *Prog. Quant. Elect.*, **21:** 1 (1997).

معدل الانبعاث الذري داخل مرنان كمي

سعود العوفي
قسم الفيزياء ، جامعة طيبة
المدينة المنورة – المملكة العربية السعودية

المستخلص. تم تقديم الصياغة العامة لدراسة معدل الانبعاث لذرة داخل مرنان كمي أسطواني ذي جودة نوعية عالية. في البدء ، قمنا – كما هو المعتاد – باشتقاق المجال الكهرومغنطيسي داخل مرنان مغلق، وذلك تمهيدا لتكمية أنماط الفجوة بداخله. وهذه التكمية بدورها تمهد لحساب الاعتماد الموضعي لمعدل الانبعاث الذري في المرنان. حيث سنجد أنه تبعا للحالات المختلفة سيزيد تارة وينقص أخرى ، بل حتى أنه قد يخمد كليا. ولابد من الإشارة هنا أن معدل الانبعاث الذري في الأنظمة ذات الأبعاد الكمية يكون ممكنا فقط لأعداد قليلة من أنماط الفجوة. وختاما نعرض الحسابات التي قد تم أخذها لذرة صوديوم موجودة في مرنان مجوف كمي الأبعاد.